INSTITUTE OF PHYSICS PUBLISHING JOURNAL OF PHYSICS: CONDENSED MATTER

J. Phys.: Condens. Matter **13** (2001) 1151–1158 www.iop.org/Journals/cm PII: S0953-8984(01)12033-3

Luminescence concentration quenching of $^1D_2$ state in YPO_4:Pr^{3+}

Houtong Chen[1,2], Rui Lian[2], Min Yin[2,4], Liren Lou[2], Weiping Zhang[2], Shangda Xia[2] and Jean-Claude Krupa[3]

[1] Structure Research Laboratory, University of Science and Technology of China, 230026 Hefei, People's Republic of China
[2] Department of Physics, University of Science and Technology of China, 230026 Hefei, People's Republic of China
[3] Institut de Physique Nucleaire, 91406 Orsay Cedex, France

E-mail: yin@ipno.in2p3.fr

Received 22 February 2000, in final form 7 December 2000

Abstract

Under selective excitation of the $^3P_0$ level of the Pr^{3+} ion in YPO_4, the emission spectra and fluorescence decay curves were measured at different concentrations and temperatures. The origin of the spectral line located at 16 318 cm^{-1} (612.8 nm) was discussed and attributed to the $^1D_2 \rightarrow {}^3H_4$ transition. The process of concentration quenching for the $^1D_2$ state was also studied. Using the Inokuti–Hirayama model, the non-exponential fluorescence decay curves of the $^1D_2$ level were fitted. The result shows that dipole–quadrupole interaction between Pr^{3+} ions, which causes $^1D_2 \rightarrow {}^1G_4$ and $^3H_4 \rightarrow {}^3F_4$ cross-relaxation, results in the quenching of $^1D_2$ emissions.

1. Introduction

Lanthanide orthophosphate is a good host for a lot of reasons. For example, it is used as a candidate for the storage of long-term radioactive actinide wastes [1]. Accordingly, a series of investigations of chemical and physical properties for lanthanide orthophosphate have been in progress in recent decades [2–4]. The trivalent ion Pr^{3+} has attracted considerable attention in recent years for the interesting fluorescence features such as upconversion [5–7] and UV emission [8]. Energy transfer and concentration quenching of luminescence have been studied recently in Pr^{3+} doped crystals [9–12], powder samples [13] and some glasses [7, 14, 15]. The results show that among the mechanisms responsible for the concentration quenching of Pr^{3+} emission, cross-relaxation is important.

YPO_4 is known to have the zircon structure with space group D_{4h}^{19}. In YPO_4:Pr^{3+}, Pr^{3+} substitutes Y^{3+} in a site of D_{2d} symmetry. The spectroscopic study of the Pr^{3+} ion with the $4f^2$ configuration in YPO_4 can be used to simulate the electronic structure of actinide ions with $5f^2$ configuration such as U^{4+}. There have not been many reports on luminescence properties

[4] Author to whom correspondence should be addressed.

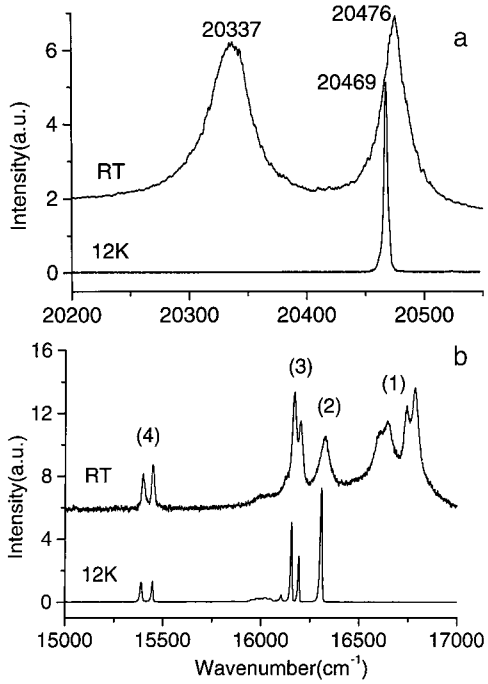

Figure 1. (a) Excitation spectra monitoring at $^3P_0 \rightarrow {}^3H_6$ emission and (b) emission spectra of YPO_4:Pr^{3+} (1 mol%) at room temperature and 12 K. The numbers (1), (2), (3) and (4) correspond to the transitions of $^1D_2 \rightarrow {}^3H_4$, $^1D_2(\Gamma_3) \rightarrow {}^3H_4(\Gamma_5)$, $^3P_0 \rightarrow {}^3H_6$ and $^3P_0 \rightarrow {}^3F_2$ respectively.

of YPO_4:Pr^{3+} and the previous studies concerned mainly the energy levels of $4f^2$ and 4f5d configurations [4, 8]. Naik *et al* studied the concentration quenching of fluorescence from the $^1D_2$ state of Pr^{3+} in YPO_4 by measuring decay times at different concentrations [16]. But there is still a need to understand the interaction that results in the concentration quenching.

In this work, we present the spectroscopic studies on YPO_4:Pr^{3+} at different temperatures and concentrations. The mechanism of concentration quenching of $^1D_2$ emission is discussed.

2. Experimental details

Pr^{3+} doped YPO_4 powder samples with concentration varying from 0.01 to 10 mol% were prepared from the starting materials Pr_6O_{11}, Y_2O_3 and $(NH_4)_2HPO_4$ by the precipitation method. The excitation spectra monitoring at $^3P_0 \rightarrow {}^3H_6$ emission were recorded at room temperature and 12 K with a frequency-tripled YAG:Nd^{3+} laser-pumped dye laser as a excitation source, and the dye used here was Coumarin 500. Under the selective excitation of the $^3P_0$ level of the Pr^{3+} ion, the emission spectra both originating from $^3P_0$ and $^1D_2$ levels of the Pr^{3+} ion were recorded using a GDM-1000 Carl Zeiss grating double monochromator at room temperature and 12 K. Using above procedures the emission spectra were also recorded at different concentrations with the same measuring conditions. The fluorescence decay curves were recorded at 12 K by using a Lecroy model 9410 oscilloscope interfaced with a computer.

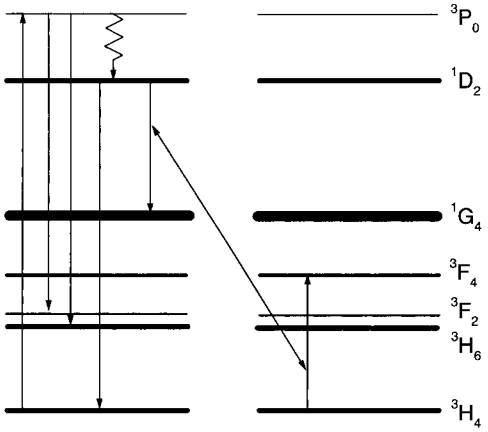

Figure 2. The energy levels and related transition diagram for Pr^{3+} in YPO_4.

3. Results and discussion

The excitation spectra of $^3P_0 \rightarrow {}^3H_6$ emission of Pr^{3+} doped YPO_4 (with 1 mol% Pr concentration) are shown in figure 1(a). At room temperature, there are two excitation peaks located at 20 337 and 20 476 cm^{-1}, and the separation 139 cm^{-1} is consistent with the lower Stark level Γ_5 and the lowest Stark level Γ_4 of the ground state $^3H_4$. While only one sharp peak located at 20 469 cm^{-1} appears at 12 K. For an ion with even number of electrons such as Pr^{3+} ($4f^2$), the crystal field eigenstates carry the Γ_1–Γ_5 point group representations associated with D_{2d} site symmetry. A full analysis of the Pr^{3+} absorption and level scheme is given in [4]. We will follow the interpretation of [4]. Selection rules for the allowed electric dipole transitions reduce to

$$\Gamma_4(\Gamma_3) \leftrightarrow \Gamma_1(\Gamma_2)$$
$$\Gamma_5 \leftrightarrow \Gamma_1, \Gamma_2, \Gamma_3, \Gamma_4, \Gamma_5.$$

At room temperature all the Stark levels of the $^3H_4$ state are populated. According to the selection rules, the transitions $^3H_4(\Gamma_4, \Gamma_5) \rightarrow {}^3P_0(\Gamma_1)$ are allowed, so there are two peaks in the excitation spectrum at room temperature. The 20 337 cm^{-1} line is attributed to the $^3H_4(\Gamma_5) \rightarrow {}^3P_0$ transition, and the 20 476 cm^{-1} line is for the $^3H_4(\Gamma_4) \rightarrow {}^3P_0$ transition. At 12 K, only the Γ_4 level is populated, therefore only the peak located at 20 469 cm^{-1} corresponding to the transition of $^3H_4(\Gamma_4) \rightarrow {}^3P_0$ is recorded. It should be pointed out that the frequency of $^3H_4(\Gamma_4) \rightarrow {}^3P_0$ transition shifts to the red side at 12 K compared with that at room temperature.

Figure 1(b) is the emission spectra of YPO_4:Pr^{3+} under selective excitation of the $^3P_0$ state. It is composed of four groups of lines, which correspond to transitions of (1) $^1D_2(\Gamma_1, \Gamma_5) \rightarrow {}^3H_4(\Gamma_4, \Gamma_5)$, (3) $^3P_0(\Gamma_1) \rightarrow {}^3H_6(\Gamma_4, \Gamma_5)$ and (4) $^3P_0(\Gamma_1) \rightarrow {}^3F_2(\Gamma_4, \Gamma_5)$ respectively. The energy levels and related transition diagram for Pr^{3+} in YPO_4 is presented in figure 2 with low resolution. The emission line of group (2) (16 318 cm^{-1}) was presumably assigned to be the $^1D_2(\Gamma_3) \rightarrow {}^3H_4(\Gamma_5)$ transition [4]. The facts that the transitions of group (1) and group (2) have the same lifetimes and their emission intensities have the same concentration dependence (figure 3) support the assignment. According to the assignment the $^1D_2(\Gamma_3)$ level is located at 16 457 cm^{-1} above the ground state, but there is no observation for the corresponding line in the absorption spectrum. This can be explained as follows. The populations of the

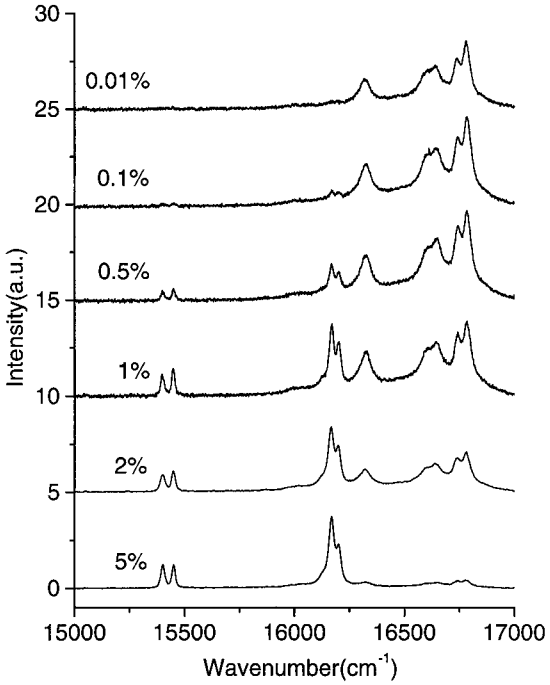

Figure 3. Emission spectra of YPO_4:Pr^{3+} with different concentrations at room temperature under $^3P_0$ excitation at 20 337 cm^{-1}.

Stark levels obey the Boltzmann distribution law. There are 283 cm^{-1} and 331 cm^{-1} energy separation between $^1D_2(\Gamma_3)$ and $^1D_2(\Gamma_5)$, $^1D_2(\Gamma_1)$ respectively, so at room temperature, the population of the $^1D_2(\Gamma_3)$ level is twice and five times those at $^1D_2(\Gamma_5)$ and $^1D_2(\Gamma_1)$ levels. But the fluorescence intensity originating from $^1D_2(\Gamma_3)$ is weaker than those originating from $^1D_2(\Gamma_1, \Gamma_5)$ levels (figure 1(b)). This means that the transition rate of $^1D_2(\Gamma_3)$ is much smaller than those of $^1D_2(\Gamma_1, \Gamma_5)$ levels. This may help to understand why the $^3H_4(\Gamma_5) \rightarrow {}^1D_2(\Gamma_3)$ absorption should be weak and hardly observed even at room temperature. At low temperature, the population via non-radiative relaxation from the $^3P_0$ state concentrates at the lowest $^1D_2(\Gamma_3)$ level, which results in the disappearance of the first group emission lines.

The emission spectra with different Pr^{3+} concentrations are shown in figure 3. When the Pr^{3+} concentration is low, though the $^3P_0$ level is selectively excited, only $^1D_2$ emissions are left. This means that the non-radiation relaxation rate from $^3P_0$ to $^1D_2$ levels is quite large. Raman and infrared spectra of YPO_4 show that the distribution of phonon energy [2] extends to about 900–1000 cm^{-1}. Only four phonons are needed to match up the energy difference between $^3P_0$ and $^1D_2$ levels (about 4000 cm^{-1}). This causes the effective non-radiation relaxation from $^3P_0$ to $^1D_2$ levels.

The concentration dependence curves for $^3P_0$ and $^1D_2$ emissions are shown in figure 4, from which we can see that $^3P_0$ and $^1D_2$ emissions are different in concentration dependence. When the Pr^{3+} concentration is very low, the fluorescence intensities originating from $^3P_0$ and $^1D_2$ levels both increase linearly with increasing concentration. Concentration quenching does not occur at low concentration; this is because in this condition the average distance among the Pr^{3+} ions is so large that the interaction is very weak. So the fluorescence intensities of $^3P_0$ and $^1D_2$ emissions both increase linearly as Pr^{3+} concentration increases in the very low

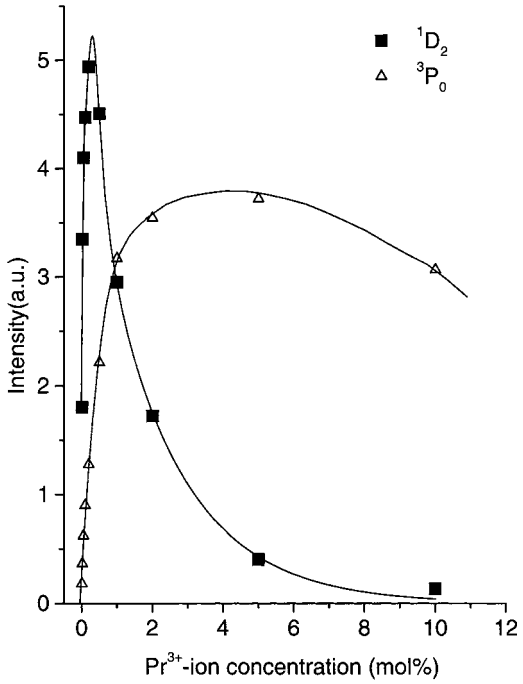

Figure 4. Fluorescent intensity of $^3P_0$ and $^1D_2$ states against Pr^{3+} concentration in YPO_4.

concentration range. As the concentration rises further, the fluorescence intensities of $^1D_2$ and $^3P_0$ levels also increase but not linearly, and reach their maximum at about 0.3 mol% for $^1D_2$ and 3 mol% for $^3P_0$ respectively, then decrease. Almost no fluorescence from the $^1D_2$ level is observed for the 10 mol% Pr^{3+} concentration sample. The quenching concentration agrees very well with the value reported by Naik *et al* [16], where they got it by measuring the fluorescence lifetimes of $^1D_2$ emission at different Pr^{3+} concentrations. Figure 4 also tells us that the $^1D_2$ emissions quench much faster than those of $^3P_0$. This means that, compared with the $^3P_0$ level, the interaction causing $^1D_2$ concentration quenching is stronger and depends much more on the distance among Pr^{3+} ions.

Figures 5(a) and (b) give the fluorescence decay of $^3P_0$ and $^1D_2$ emissions under selective excitation of the $^3P_0$ level at 12 K, with Pr^{3+} concentrations of 1 mol% and 6.2 mol% respectively. The fluorescence decays are single exponential for the $^3P_0$ level with almost the same lifetime of about 0.66 μs at 1 mol% and 6.2 mol% Pr^{3+} concentrations (figure 5(a)), while for the $^1D_2$ level the fluorescence decays obviously depart from single exponential, and the decay rate is much larger for 6.2 mol% than for 1 mol% (figure 5(b)). But when the time is long enough, both of the fluorescence decays for 1 mol% and for 6.2 mol% are nearly single exponential, and they give nearly the same lifetime, about 52 μs, which is much longer than that of the $^3P_0$ level. From the fluorescence decay curves we may get some information responsible for the concentration quenching of the $^1D_2$ state fluorescence.

Usually, there are two mechanisms for concentration quenching: (1) cross-relaxation between Pr^{3+} ions and (2) excitation energy migration among donors until quenched by cross-relaxation or reaching some killers [17]. We can neglect D–D migration of the $^1D_2$ level among different Pr^{3+} ions for the following reasons. At 12 K, among the Stark levels of the $^1D_2$ state only the Γ_3 level has population, and among the Stark levels of the $^3H_4$ state only the

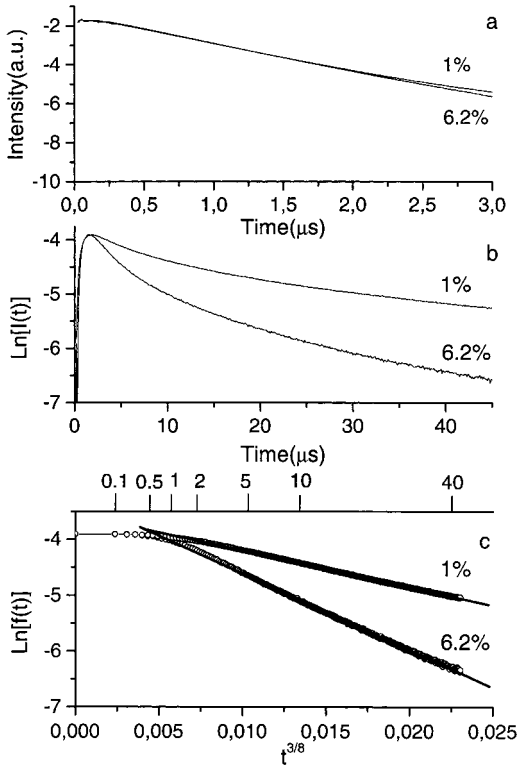

Figure 5. Fluorescence decay curves of (a) $^3P_0$ and (b) $^1D_2$ states of YPO_4:Pr^{3+} (1 mol% and 6.2 mol% Pr^{3+} ion concentrations) under $^3P_0$ excitation at 12 K; (c) the $^1D_2$ decay curves were fitted using equation (2) with $s = 8$ after deducting the intrinsic transition. Here the point where the intensity had the maximum value was defined as the original point of time.

lowest, Γ_4, has population. Because the transition between Γ_3 and Γ_4 is forbidden according to the selection rules, when the Pr^{3+} ion is de-excited from $^1D_2(\Gamma_3)$ to one of the allowed Stark levels of the $^3H_4$ state, the other Pr^{3+} ions nearby remaining in the ground state $^3H_4(\Gamma_4)$ cannot be excited because of the energy mismatch. Therefore the D–D migration can be neglected and the first mechanism will dominate the concentration quenching process. Energy transfer is caused by the electronic multipolar interactions between Pr^{3+} ions; the Inokuti–Hirayama model [18]

$$I(t) = I(0)\exp\left[-\frac{t}{\tau_r} - Ct^{3/s}\right] \tag{1}$$

can be used to discuss the energy transfer and concentration quenching of the $^1D_2$ level, where $s = 6$, 8 and 10 denote dipole–dipole, dipole–quadrupole and quadrupole–quadrupole interactions respectively, τ_r is the intrinsic fluorescence lifetime of $^1D_2(\Gamma_3) \rightarrow {}^3H_4(\Gamma_5)$ and C is a parameter containing the A concentration (C_A) and the D–A interaction strength.

It is reasonable to consider the lifetime 200 μs [16] as the intrinsic fluorescence lifetime τ_r of the $^1D_2$ level, which is measured at very low concentration (0.01 mol%). If the intrinsic fluorescence is deducted, equation (1) changes to

$$f(t) = f(0)\exp[-Ct^{3/s}]. \tag{2}$$

This is the decay caused by the D–A transfer, and the $\ln[f(t)] - t^{3/s}$ curve should be a straight line if the interaction is dominated by one of those three kinds of electric multipolar interaction. Firstly, using equation (2) the experimental fluorescence decay curve at 1 mol% Pr^{3+} concentration was fitted. Here the point where the intensity had the maximum value was defined as the original point of time. This is because the population at the $^1D_2$ level comes from the $^3P_0$ level via non-radiative relaxation and has a rising process. Compared with the fluorescence decay of the $^1D_2$ level, the rising process is so fast that we can still consider the $^1D_2$ level is excited equably when the intensity reaches its maximum. We found that a perfect $\ln[f(t)] - t^{3/m}$ straight line could be obtained for $s = 8$ while $t > 1$ μs (figure 5(c)). For $t < 1$ μs, the fit departs from linear obviously, which is clearly due to the non-radiative relaxation from $^3P_0$ to $^1D_2$, although it has become weaker. The fit shows that the dipole–quadrupole interaction ($s = 8$) is the main process for the D–A energy transfer, which results in the concentration quenching of Pr^{3+} ions in relative heavily doped samples.

Energy level structure [4] tells us that the energy difference between $^1D_2$ and $^1G_4$ matches closely with that between $^3H_4$ and $^3F_4$, so the cross-relaxation can process easily between Pr^{3+} ions, shown in figure 2. For example, $^1D_2(\Gamma_3) \rightarrow {}^1G_4(\Gamma_1)$ (6842 cm^{-1}), which is electric dipole (ED) forbidden but electric quadrupole allowed, is near resonant with the $^3H_4(\Gamma_4) \rightarrow {}^3F_4(\Gamma_5)$ (6829 cm^{-1}, ED allowed). In addition, the lifetime of the $^1D_2$ level is much longer than that of the $^3P_0$ level, which also is favourable to the cross-relaxation process. The energy transfer rate caused by electric dipole–quadrupole interaction is proportional to $(1/r)^8$. It is sensitive to the Pr^{3+} concentration and leads to the strong fluorescence intensity dependence on concentration for $^1D_2$ emission.

Using equation (2) and with the same procedures as in the case of 1 mol%, the experimental fluorescence decay curve at 6.2 mol% Pr^{3+} concentration was fitted too. We found that $\ln[f(t)] - t^{3/m}$ curve also was a straight line while $t > 1$ μs (figure 5(c)) for $s = 8$, just the result we had expected. This supports our conclusion that the electric dipole–quadrupole interaction between Pr^{3+} ions is the main interaction responsible for the concentration quenching of $^1D_2$ fluorescence in $YPO_4:Pr^{3+}$.

4. Conclusion

The luminescence of Pr^{3+} doped YPO_4 has been analysed. The origin of the 16 318 cm^{-1} (612.8 nm) line is discussed and is confirmed to be the $^1D_2(\Gamma_3) \rightarrow {}^3H_4(\Gamma_5)$ transition. Using the Inokuti–Hirayama model the fluorescence decay curves of the $^1D_2$ level have been fitted. The result shows that the dipole–quadrupole interaction between Pr^{3+} ions, which causes $^1D_2 \rightarrow {}^1G_4$ and $^3H_4 \rightarrow {}^3F_4$ cross-relaxation, results in the quenching of $^1D_2$ emissions.

Acknowledgment

This work was supported by the National Natural Science Foundation of China (19774052).

References

[1] Boatner L A *et al* 1980 *The Scientific Basis For Nuclear Waste Management* vol 2, ed C J Northrup (New York: Plenum) p 289
[2] Begun G M, Beall G W, Boatner L A and Gregor W J 1981 *J. Raman Spectrosc.* **11** 273
[3] Rappaz M, Abraham M M, Ramey J O and Boatner L A 1981 *Phys. Rev.* B **23** 1012
[4] Hayhurst T, Shalimoff G, Conway J G, Edelstein N, Boatner L A and Abraham M M 1982 *J. Chem. Phys.* **76** 3960

[5] Koch M E, Kueny A W and Case W E 1990 *Appl. Phys. Lett.* **56** 1083
[6] Schäfer U, Neukum J, Bodenschatz N and Heber J 1994 *J. Lumin.* **60/61** 633
[7] Balda R *et al* 1999 *J. Non-Cryst. Solids* **256/257** 299
[8] Zhang W, Yin M, Zhang J and Mayoley A 1996 *Chin. J. Lumin.* **17** 129
[9] Mazurak Z G, Van Vliet J P M and Blasse G 1987 *J. Solid State Chem.* **68** 227
[10] Savoini B, Santiuste J E M and González R 1997 *Phys. Rev.* B **56** 5856
[11] Balda R *et al* 1999 *Phys. Rev.* B **59** 9972
[12] Voda M *et al* 1998 *J. Alloys Compounds* **277** 214
[13] Donega C D *et al* 1995 *J. Phys. Chem. Solids* **56** 267
[14] Balda R *et al* 1999 *Opt. Mater.* **13** 159
[15] Balda R *et al* 1999 *J. Phys.: Condens. Matter* **11** 7411
[16] Naik R C, Karanjikar N P and Razvi M A N 1992 *J. Lumin.* **54** 139
[17] Blasse G 1988 *Prog. Solid State Chem.* **18** 79–171
[18] Inokuti M and Hirayama F 1965 *J. Chem. Phys.* **43** 1978